Engineering Structures 202 (2020) 109812

Contents lists available at ScienceDirect

Engineering Structures

journal homepage: www.elsevier.com/locate/engstruct

Propagation and quantification of uncertainty in the vulnerability estimation of tall concrete bridges

Farahnaz Soleimani

School of Civil and Environmental Engineering, Georgia Institute of Technology, Atlanta, GA 30332, United States

ARTICLE INFO

Keywords:
Uncertainty quantification, vulnerability analysis
Probabilistic seismic demand model
Concrete box-girder bridge
Seismic response
Fragility curve
Tall bridge
Geometric irregularities
Irregular bridges

ABSTRACT

Bridges are critical links in a transportation network, and their seismic vulnerability can lead to substantial economic losses, particularly the ones located in high-risk seismic zones. Bridge vulnerability can be assessed by developing fragility curves that indicate the probability of reaching or exceeding a specific level of damage. Past earthquakes have revealed a high likelihood to experience seismic damage for bridges with irregularities in their configurations. Since the research on the seismic reliability of irregular bridges with consideration of uncertainty is limited, this paper aims to address this deficiency by analyzing the impacts of typical sources of uncertainties including ground motion, material, and geometric attributes on the vulnerability of tall and normal box-girder concrete bridges. This study compares the fragility of considered cases by performing nonlinear time history analysis of representative bridges and developing probabilistic seismic demand models in order to generate the corresponding fragility curves. During this process, the influence of each type of uncertainty is investigated through statistical analysis of the bridge responses. The findings demonstrate a noticeable seismic risk of tall bridges compared to the normal ones, and among the evaluated categories, the uncertainties associated with the geometric attributes showed the highest influence on the seismic demands.

1. Introduction

Fragility analysis, which leads to the development of fragility curves, is a prominent approach for damage assessment of various components of a bridge exposed to a seismic hazard. For each bridge, these curves predict the extent of probable damage caused by an earthquake, as well as the conditional probability of damage as a function of ground motion intensity. In this regard, researchers typically propose empirical [1] and analytical [2] fragility curves for regular, straight bridges. Empirical approaches can be used only when sufficient earthquake records are available. Thus, when sufficient records are not available, the analytical approach is commonly applied. Analytical fragility curves were created initially by Yu, et al. [3] and further extended by Hwang, et al. [4], Gardoni, et al. [5], and Zhong, et al. [6]. In the past two decades, the development of analytical fragility curves [7,8,2,9,10,11,12] has been an essential step towards the risk assessment of the existing highway transportation network. However, presently, there is limited research on the seismic fragility analysis of bridges with irregularities or inconsistencies in their configuration.

The experiences of previous earthquakes, such as the Northridge earthquake in California in 1994, the Kobe earthquake in Japan in 1995, and the earthquake off the coast of central Chile in 2010, reveal that bridges with irregularities in their configurations have a higher chance of collapsing or sustaining severe damage than bridges constructed with typical configurations [13,14,15,16]. Bridges with typical geometric configurations are defined as straight bridges with zero skew angle, zero curvature, with normal column heights, and balanced stiffness between frames. Bridges with geometric irregularities are typically constructed in specific regions with complex topography of the foundation layout, such as mountainous areas, deep valleys, or overcrossings. Consequently, based on the topography attributes, some of these bridges have columns higher than the typical range, while others have columns of variable height. At present, there is very limited research on this topic; hence, there is a need to assess the seismic performance of these irregular bridge configurations further.

Utilizing post-earthquake observations, Zheng & Wenhua [17] explored the four primary damage states of bridges with high or non-uniform columns in mountainous areas. Based on their study, the first damage state was associated with changes in the position of the abutment, abutment settlement, and damage to the superstructure deck. The second damage state was mainly related to the cracking and breaking of piers, in addition to the buckling of the steel reinforcement. The inclination and deterioration of supports caused the third damage state; the final damage state resulted in bridge collapse because of the failure of piers and supports, followed by the falling of the superstructure. Zheng & Wenhua [17] also clarified the importance of following a

E-mail address: soleimani@gatech.edu.

https://doi.org/10.1016/j.engstruct.2019.109812
Received 5 April 2019; Received in revised form 16 September 2019; Accepted 15 October 2019
Available online 06 November 2019
0141-0296/

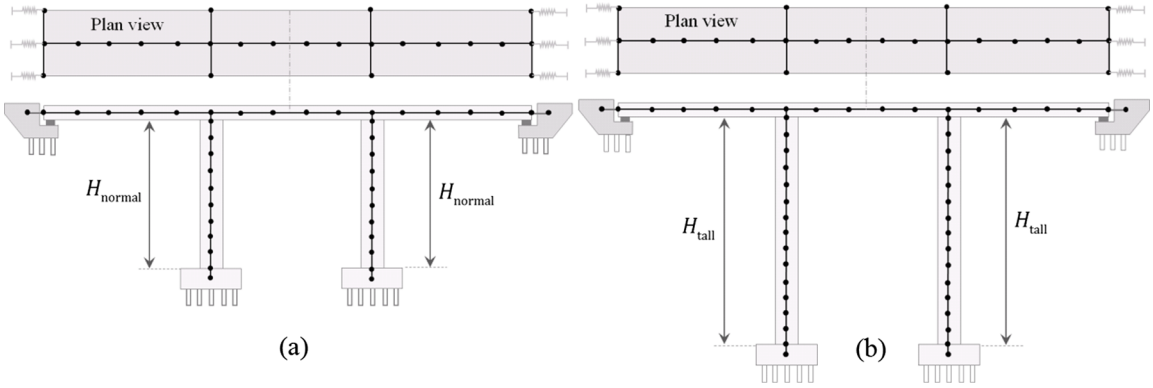

Fig. 1. Schematic diagram of regular and irregular bridge layout: (a) regular and (b) tall bridges.

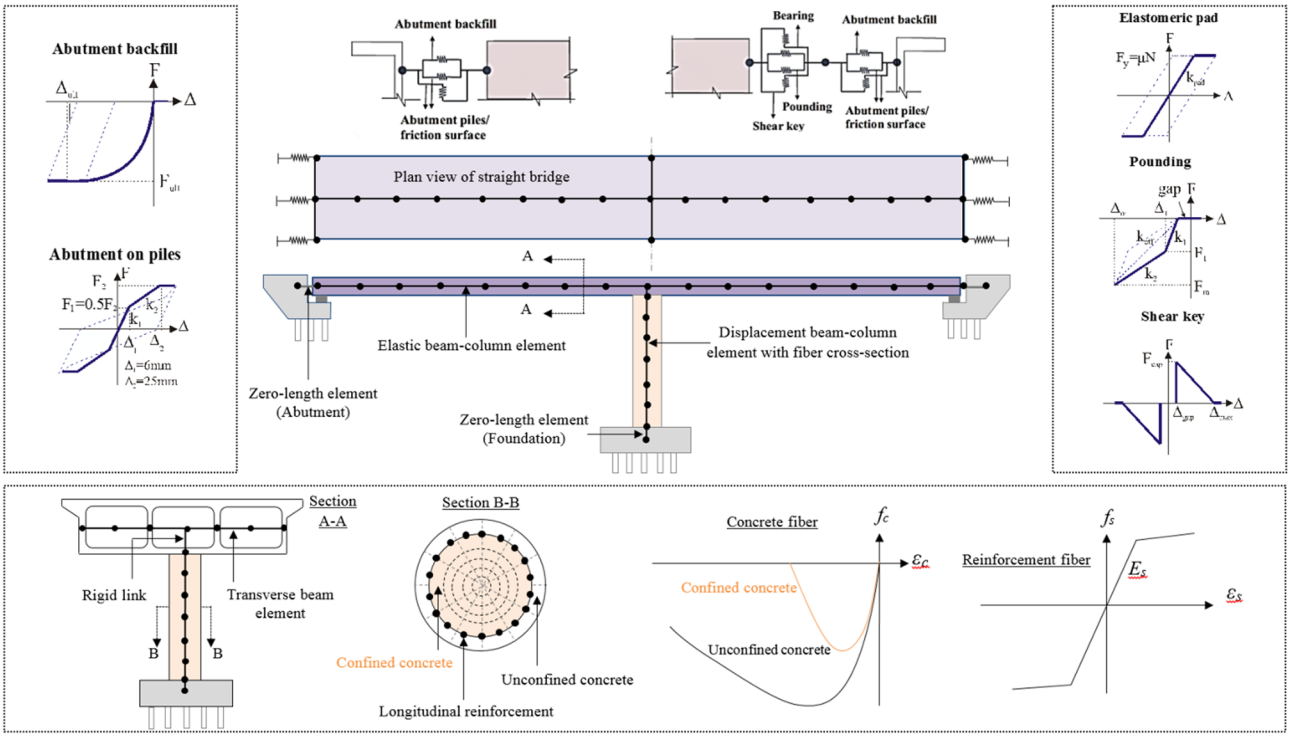

Fig. 2. Schematic diagram of the numerical modeling of a single-frame, two-span, box-girder bridge, and the cross-sectional view of the bridge deck.

Table 1
The assigned nomenclature for irregular bridges.

Nomenclature	Geometric Irregularity	Range of irregular parameter	Parameter bounds
MTL	Tall column bents	Moderately tall	$1.5 \leq H_{ave_{tall}}/H_{ave_{normal}} < 2.5$
VTL		Very tall	$2.5 \leq H_{ave_{tall}}/H_{ave_{normal}} < 3.5$
ExTL		Extremely tall	$3.5 \leq H_{ave_{tall}}/H_{ave_{normal}} < 4.5$

separate seismic design procedure for tall-pier bridges. They recommended using stronger column bents to resist large bending moments, shear forces, and torques. All of these factors indicate the complex seismic response of bridges with unconventional column

Table 2
Lognormal distribution parameters for the column height according to the bridge inventory (also found in Soleimani, et al. [28]).

Parameter	Design era	Min	Max	Mean	Standard deviation
Normal column heights ($H_{ave_{normal}}$)	Pre-1971	5.0 (m)	8.6 (m)	1.880	−1.050
	1971–1990	5.0 (m)	10.0 (m)	1.959	−1.016
	Post-1990	5.1 (m)	11.3 (m)	2.031	−0.990
Ratio for tall column heights ($H_{ave_{tall}}/H_{ave_{normal}}$)	Pre-1971	0.56	4.56	0.715	0.267
	1971–1990	0.65	4.17	0.729	0.237
	Post-1990	0.49	3.97	0.697	0.232

Table 3
Distribution of modeling parameters (also found in Soleimani, et al. [28]).

Parameter	Unit	Distribution	Distribution parameters	
			Factor 1*	Factor 2**
Span length	(m)	Empirical	35.0	12.3
Deck width	(m)	Empirical	20.5	12.9
Girder spacing	(cm)	Empirical	289.6	100.1
Top flange thickness	(cm)	Empirical		
Reinforced concrete			21.3	2.8
Pre-stressed concrete			20.8	2.5
Bottom flange thickness	(cm)	Uniform	11.4	16.5
Wall thickness	(cm)	Uniform	25.4	30.5
Depth of superstructure	(cm)	Uniform		
Reinforced concrete		Uniform	0.055* Span length	0.06* Span length
Pre-stressed concrete		Uniform	0.04* Span length	0.045* Span length
Column diameter	(cm)	Randomly assign 50% of simulation to each 168 and 183		
Longitudinal reinforcement ratio	N/A	Uniform		
Pre-1970 design era			1.4	2.4
1970–1990 design era			1.0	3.7
Post-1990 design era			1.0	3.5
Confinement ratio	N/A	Uniform		
Pre-1970 design era			Spacing: 30.5 cm	
1970–1990 design era			0.3	0.9
Post-1990 design era			0.4	1.7
Abutment backwall height	(m)	Uniform	1.1	2.6
Pile spacing	(m)	Uniform	1.7	2.1
Foundation translational stiffness	(kN/cm)	Normal		
Single column − 6 ft dia column 1% long. steel			2977.2	1401.0
Single column − 6 ft dia column 3% long. steel			2451.8	1050.8
Foundation rotational stiffness	(kN-m/rad)	Normal		
Single column − 6 ft dia column 1% long. steel				
Single column − 6 ft dia column 3% long steel			4632.4	1355.8
			7344.0	1129.8
Concrete compressive strength	(Mpa)	Normal	34.5	4.3
Reinforcing steel yield strength	(Mpa)	Lognormal	6.14	2.0
Shear key capacity	(kN)	Normal	4884.2	646.8
Multiplicative factor for coefficient of friction of bearing pads	N/A	Lognormal	0	0.1
Shear modulus of elastomeric bearing pads	(Mpa)	Uniform	551.6	1723.9
Transverse gap between deck and shear keys	(mm)	Uniform	0	38.1
Longitudinal gap between deck and abutment	(mm)	Uniform	0	152.4
Pile stiffness	(kN/cm)	Lognormal	80.6	0.86
Mass factor	N/A	Uniform	1.1	1.4
Damping	%	Normal	0.045	0.0125

*, ** Factors 1 and 2 represents the mean and standard deviation for normal, lognormal, and empirical distributions; lower bound and upper bound for uniform distribution.

Table 4
The common list of recorded engineering demand parameters.

Component	Engineering demand parameter	Notation	Units
Columns	Curvature ductility	ϕ_c	1/mm
Deck	Displacement	δ_{deck}	mm
Foundation translation	Displacement	δ_{fnd}	mm
Passive abutment response	Displacement	δ_p	mm
Active abutment response	Displacement	δ_a	mm
Transverse abutment response	Displacement	δ_t	mm

attributes.

Probability-based methods are commonly used to deal with uncertainties that are inherently involved in the performance analysis of structural systems. Identifying and considering relevant uncertain factors is crucial for the proper handling of uncertainty in a probabilistic analysis approach [18,19,20]. In this regard, there is a need to promote further research for treating various sources of uncertainties, including aleatory and epistemic, in the seismic performance analysis of bridges. Epistemic uncertainty results from lack of information or insufficient data [21]. Improving available data and modeling strategies by inspecting the properties of existing structures helps to reduce epistemic sources of uncertainty and hence improve the accuracy of predictive probabilistic models [22,23,24].

There are only a few studies that explored the uncertainty quantification in developing probabilistic seismic demand models and fragilities of bridges. Mackie and Nielson [25] studied a five-span box-girder bridge in California. They assessed the effect of nine uncertain modeling variables of bridge columns on the column's fragility curves based on four different cases. The considered variables were mostly related to the material properties of the bridge columns. Lei Wang et al. [26] proposed a fuzzy method to evaluate the reliability of aging RC

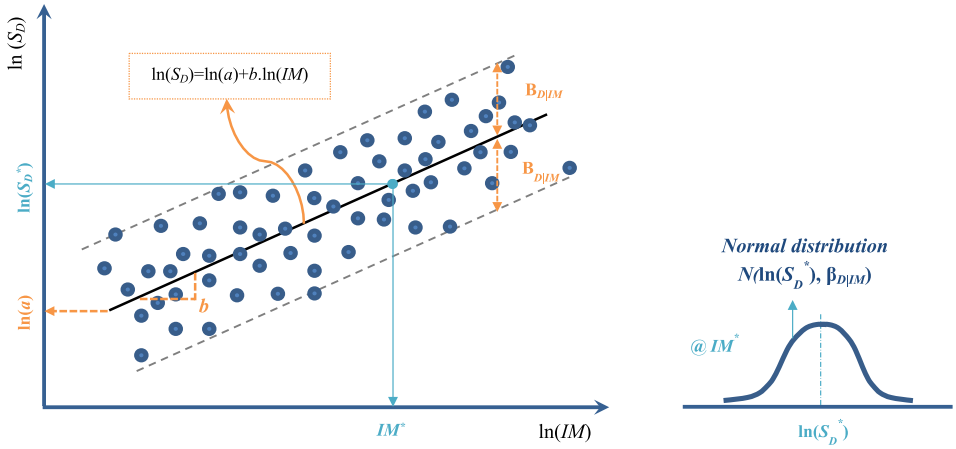

Fig. 3. Illustration of a typical PSDM in the transformed space.

Table 5
Description of abbreviations used for the sources of uncertainty.

Abbreviation	Description
GM	Ground Motions
GEO	Geometric Parameters (e.g. Column height, Span Length)
MAT	Material Properties (e.g. Concrete strength)
OTHERS	Additional Modeling Features (e.g. Damping Ratio)

structures having data deficiency. They provided an example for an RC bridge to show that their suggested methodology is comparable with the common classic strategy and for the multimodal PDF provides higher accuracy than the classical approach. Since there is currently limited research in the sensitivity of bridge responses to the input modeling variables, the current work aims to address this deficiency by focusing on the impact of major sources of uncertainties on the seismic performance of concrete box-girder bridges with normal and tall column heights. Soleimani et al. [27] applied statistical techniques including Lasso regression to develop seismic demand models for irregular bridges (i.e., bridges with skewed abutments, tall columns, and unbalanced stiffness frames). These optimized approaches provide the most predictive models while detecting the most influential parameters on the bridge seismic responses. A quantitative measure of the uncertainty that is involved in the process of developing probabilistic seismic demand models and the fragility curves was missing in the work by Soleimani et al. [27]. Therefore, a separate study is needed to solely focus on this issue and address this deficiency. Also, the seismic response and performance of tall bridges have not been deeply studied, and hence there is a need to further assess the seismic performance of this irregular bridge configuration. The current paper aims to show how different categories of uncertainty in the modeling and analysis can affect the uncertainty in the bridge response. Moreover, the current paper provides insights regarding the differences between the performance of tall and normal bridges and the fragility of the class of tall bridges.

The intent (main objective) of this paper is to investigate the contributions of the main categories of uncertainties and their propagation, through different levels of bridge elevation, which has not been performed rigorously to date. This study investigates the quantification of uncertainties associated with the prediction of the seismic performance of concrete bridges. For this purpose, the analytical damage fragility methodology that is commonly used for typical bridges [28,7] is implemented since uncertainties pertaining to the bridge parameters and simulations are tractable. The methodology is demonstrated for a single-span box-girder bridge with common bridge characteristics in California. This procedure involves various sources of uncertainty arising from probabilistic seismic demand analysis and Latin hypercube bridge population sampling as well as randomness in the ground excitations. The specific sources of uncertainties to be addressed by this research are: (i) ground motion, (ii) geometric attributes, (iii) material parameters, and (iv) other features such as damping ratio. The remaining parts of the paper are organized as follows. Section 2 demonstrates the strategies and details of numerical modeling for global bridge models and their various components. Section 3 introduces the analysis of the probabilistic seismic demand models of bridges and the variations caused by the studied uncertain factors. Section 4 explains the general procedure of fragility analysis and implementation and elaborates statistical comparison of the vulnerability of tall versus normal bridges. The paper concludes in Section 5 by providing a summary of the findings and contributions of this work.

2. Bridge modeling

In this study, the finite element platform, OpenSees [29], is used to generate three-dimensional (3-D) numerical models of the considered bridge categories and their corresponding configurations. Fig. 1 demonstrates schematic diagrams of the analytical model for the regular and irregular bridge types that are considered in this study. Tall bridges (Fig. 1.b) are defined as those where the average column heights are higher than 1.5 times of the average column height of the regular bridges (i.e., $H_{ave_{tall}} > 1.5 \times H_{ave_{normal}}$, [27,28]).

For each bridge type, various components of a box-girder bridge are modeled with their specific characteristics according to the design of California bridges [28] and are then integrated to generate the global analytical model of the bridge, as illustrated in Fig. 2. The general layout of the bridge model is presented in this section however interested readers are encouraged to refer to the work by Soleimani [28] for a detailed explanation of the finite-element model. The bridge deck consists of longitudinal and transverse elements known as girder elements (Fig. 2). When a bridge is subjected to an earthquake, the superstructure typically remains elastic; hence the longitudinal deck elements and the transverse girder elements are modeled as elastic

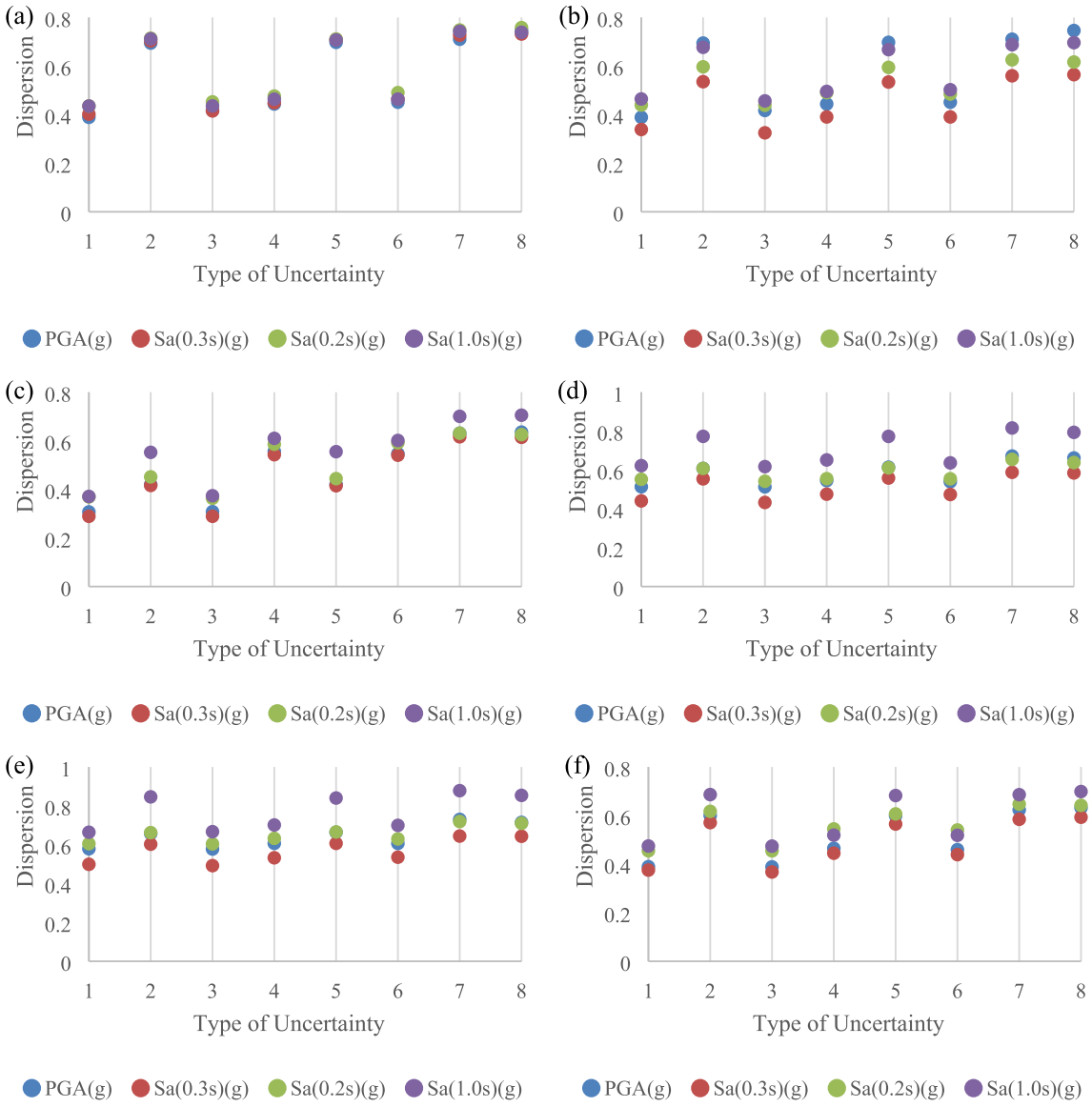

Fig. 4. Dispersion values of the captured seismic responses for the normal bridge with rigid abutment and with the uncertainty scenarios listed in Table 6; (a) column curvature, (b) deck displacement, (c) foundation translation, (d) active abutment displacement, (e) passive abutment displacement, (f) transverse abutment displacement.

beam-column elements in OpenSees with lumped masses applied on the element nodes. Transverse deck elements are connected to columns using rigid links to ensure the moment and force transfer between the deck and column. Prismatic bridge column with circular cross-section shape, which is used in the majority of the California box-girder bridges in all design eras [30,31], was selected for the consideration of this paper. In this study, single column bent (SCB) and multi-column bent (MCB) are modeled using the displacement-based nonlinear beam-column elements with fiber-defined cross-sections consisting of concrete "concrete-07" and steel reinforcement "steel-02" [32]. Different properties are considered for the confined (core) concrete and the unconfined (cover) concrete parts employing the concrete models developed by Mander, et al. [33]. The model developed by Menegotto and Pinto [34], later modified by Filippu, et al. [35], is assigned to the numerical model to add isotropic strain hardening property to the reinforcing steel. Abutments are classified as either seat or rigid diaphragm types. OpenSees' ZeroLength element is used to capture the response of the abutment backfill soil and the bi-directional forces, including abutment piles and frictional surface. The passive soil spring is modeled as a nonlinear elastic spring, as recommended by Shamsabadi and Yan [36]. The model is a function of the backwall height and the backfill soil type. Pounding or impact between the decks and/or the deck and abutment backwall is modeled using the contact element approach proposed by Muthukumar and DesRoches [37]. The other bridge components such as pounding, shear key, bearing, and piles, were modeled using the previously developed procedures.

In order to model tall bridges, the average column heights of tall bridges were normalized by the average column heights of the

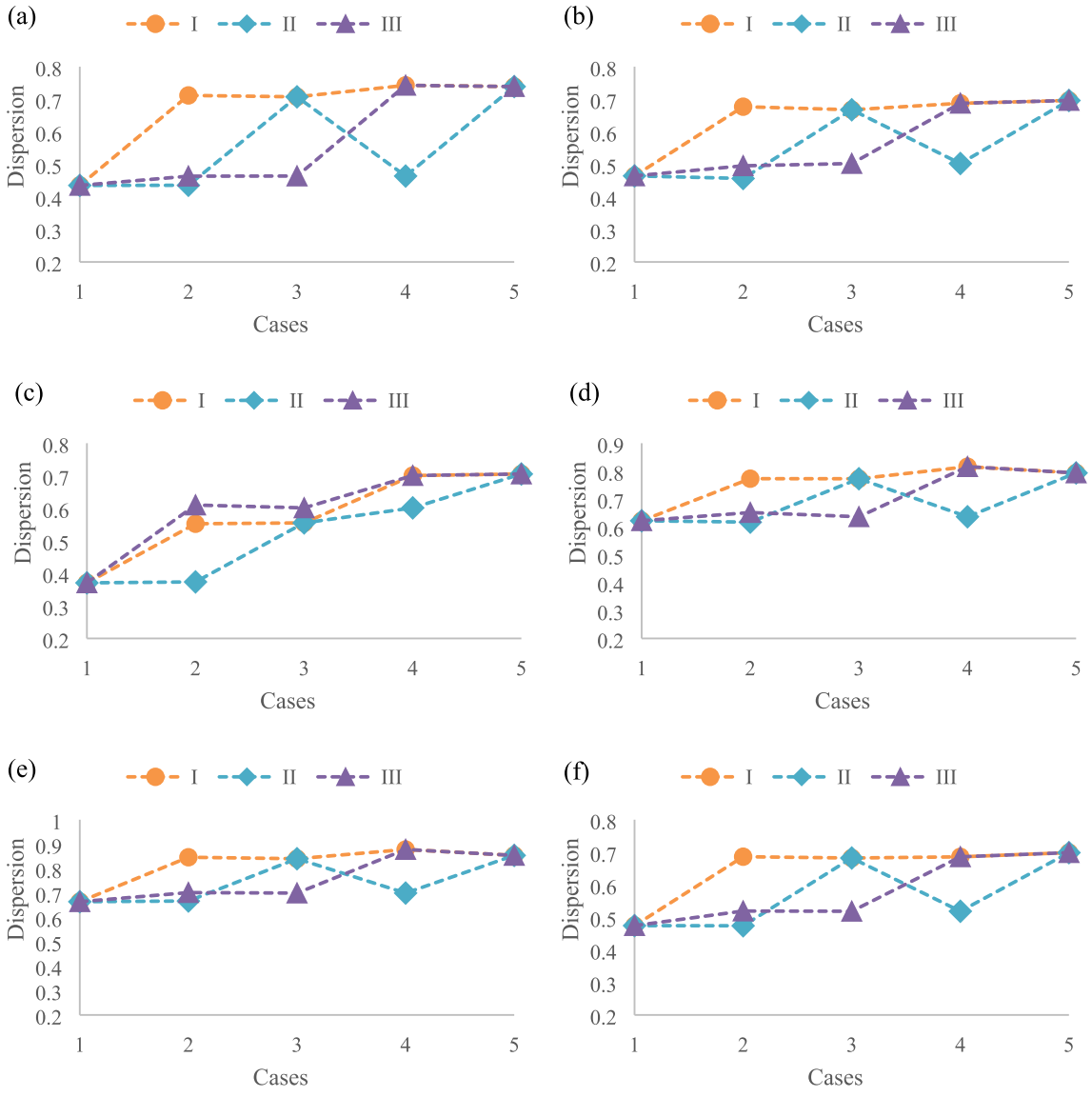

Fig. 5. Dispersion values of the captured seismic responses for the normal bridge with rigid abutment and with the uncertainty cases listed in Table 7; (a) column curvature, (b) deck displacement, (c) foundation translation, (d) active abutment displacement, (e) passive abutment displacement, (f) transverse abutment displacement.

corresponding representative regular bridges. Next, normalized-column-height values were assigned to a variable called average bridge-height ratio. Those ratios that were higher than 1.5 met the column heights criteria to be considered as tall bridges, and thus they were used for building the models for this class of bridges [27]. This study explores the seismic performance of the family of tall bridges in three ranges of column heights, as listed in Table 1. The structural modeling parameters and their associated uncertainties including probability distribution of parameters that are used to generate finite element models are listed in Table 2 and Table 3. The provided values were obtained based on reviewing the characteristics of the box-girder bridges in California.

3. Variation analysis of uncertainty in PSDMs

Performing seismic risk analysis on bridges involves several steps. The initial step includes the random pairing of an equal number of bridge samples with a suitable set of ground motions. In this study, the bridge models are subjected to a suite of recorded California ground motions (i.e., Bakers set [38]). The excitations have longitudinal and orthogonal components and are randomly oriented to the longitudinal and transverse directions of the bridge models. To consider the uncertainty associated with the modeling parameters, random bridge samples are generated utilizing the Latin Hypercube sampling technique [39] that is based on the cumulative distribution function corresponding to each of the modeling parameters.

The next steps involve performing nonlinear time history analysis

Fig. 6. Pareto plots of the bridge column response for various bridge types.

Table 6
Different scenarios for the combination* of uncertain sources in the analysis.

Scenarios	Sources of Uncertainty			
	Ground Motions	Geometric Parameters	Material Properties	Additional Modeling Features
1	●			
2	●	●		
3	●		●	
4	●			●
5	●	●	●	
6	●		●	●
7	●	●		●
8	●	●	●	●

*In each row, cells with the black circles are the uncertainty sources included in the analysis.

(NLTHA) on each bridge sample to estimate the seismic demand of the bridge components. The results of this analysis provide the peak seismic response of the specified engineering demand parameters (EDPs) (Table 4). Monitoring the key demand parameters is an essential step in the risk assessment of bridges. The EDPs are described through probabilistic seismic demand models (PSDMs); these are regression models that express the relationship between the seismic demands D and the ground motion intensities IM [40]. In this study, PGA, Sa(0.3 s), Sa (0.2 s), and Sa(1.0 s) are considered as the ground motion intensity measures. Based on the lognormal assumption [40,41], the median value of the seismic demand S_D can be estimated as a function of ground motion intensity as

$$S_D = a.\ IM^b, \tag{1}$$

where a and b are the regression coefficients that are obtained by performing a regression analysis on $D - IM$ pairs. Dispersion ($\beta_{D|IM}$) is calculated as

$$\beta_{D|IM} = \sqrt{\frac{\sum_{i=1}^{n} (\ln(D_i) - \ln(S_D))^2}{N-2}} \tag{2}$$

In Eq. (2), N shows the number of data points. It is often easier to illustrate PSDM in a transformed space (Fig. 3). Therefore, the linear representation of Eq. (1) is given by taking the natural logarithm of both sides of the equation as

$$\ln(S_D) = \ln(a) + b.\ \ln(IM) \tag{3}$$

The random input variables mentioned in Table 3 can be classified into separate categories of uncertainties based on their types. To simplify the comparison and discussion section, Table 5 assigns abbreviation to the different classes of uncertainties. Fig. 4 and Fig. 5 compare PSDM dispersion for different captured engineering demand parameters (Table 4) of the normal bridge with the rigid abutment. However, Fig. 6 displays column responses, as the most important engineering demand parameter, for different bridge types including the normal bridge with the rigid abutment, normal bridge with seat abutment, etc. Eight different scenarios, listed in Table 6, are shown in Fig. 4. In the first scenario, only the uncertainty associated with the ground motions is considered in the time history analysis. The next three scenarios represent an additional source of uncertainty. Moving from the first to the eighth scenario, the number of uncertain parameters in the bridge modeling increases.

In Fig. 4.a, comparison of the first four scenarios shows that GEO adds more variation to the column response than MAT and OTHERS. In the third and fourth scenarios which are related to adding the MAT and OTHERS to the first scenario, dispersion of the column response increases slightly. This change is a little more noticeable in scenario 4. Finally, having all sources of uncertain parameters in the eighth scenario and compare it with the first and second scenarios reveal that geometric variables in the bridge models play a major role in increasing dispersion in the seismic response of the bridge column. Fig. 5 also shows this trend. In Fig. 5.a, comparing I, II, and III (refer to Table 7 for explanation) demonstrates that the dispersion of the column response increases from case #1 to case #5. The patterns are almost similar for all the other bridge responses and also among the considered ground motion scales including PGA, Sa(0.3 s), Sa(0.2 s), and Sa(1.0 s).

It can be found from previous works on the fragility analysis of bridges [12,28] that system fragility is mostly dominated by column fragility among all the other components such as abutment type and deck that contribute to bridge vulnerability. The vertical bars in the Pareto plots of the bridge column responses (Fig. 6) represent the contribution to the dispersion of responses in rank order with the items having the highest contribution placed on the left. Therefore, evaluating scenarios 1, 2, 5, 7, and 8, clearly, GEO increases uncertainty in the column response noticeably compare to the other sources. This is true for the entire analyzed bridge classes (e.g., Fig. 6a-Normal bridge with the rigid abutment, Fig. 6b-Normal bridge with seat abutment, Fig. 6c-Tall bridge with rigid abutment and low column height ration, etc.). Also, it is seen that the pattern of the column response is very similar for all considered ground motion intensity measures (i.e., PGA, Sa(0.3 s), Sa(0.2 s), and Sa(1.0 s)). Including additional sources of uncertainty slightly changes the dispersion of the results.

The results are compared for different range of column heights in Fig. 7. For the tall bridges with rigid abutments, generally, as the column height ratio increases, the uncertainty in the results also increases (Fig. 7a). However, for the tall bridges with seat abutments, this is seen for some cases such as scenario 3, 4, and 6 and for other cases the dispersion does not have a noticeable variation across the various column height ratios.

Comparison of the dispersion of the results corresponding to the rigid and seat abutment type bridges shows that, for the tall bridges with the medium range of column heights, dispersions are almost the same for rigid and seat types. For the tall bridges with the high range of column height, cases including uncertain geometric parameters have higher values in bridges with the rigid abutments than those with the seat abutments. However, for bridges with deterministic geometric parameters, the dispersion values of rigid abutment bridges are pretty close to those of the seat abutment bridges. For normal and tall bridges with the low range of column height, dispersions of seat abutment bridges are higher than the values of the rigid abutment bridges. Overall, this shows that higher uncertainty is involved in the vulnerability analysis of seat bridge types. In general, the cases which include uncertainties associated with geometric parameters have higher dispersions.

In Fig. 8.a which corresponds to bridges with the rigid abutment,

Table 7
Various cases of combined uncertain parameters in the analysis.

Cases	I	II	III
#1	GM	GM	GM
#2	GM + GEO	GM + MAT	GM + OTHERS
#3	GM + GEO + MAT	GM + MAT + GEO	GM + OTHERS + MAT
#4	GM + GEO + OTHERS	GM + MAT + OTHERS	GM + OTHERS + GEO
#5	GM + GEO + MAT + OTHERS	GM + MAT + GEO + OTHERS	GM + OTHERS + GEO + MAT

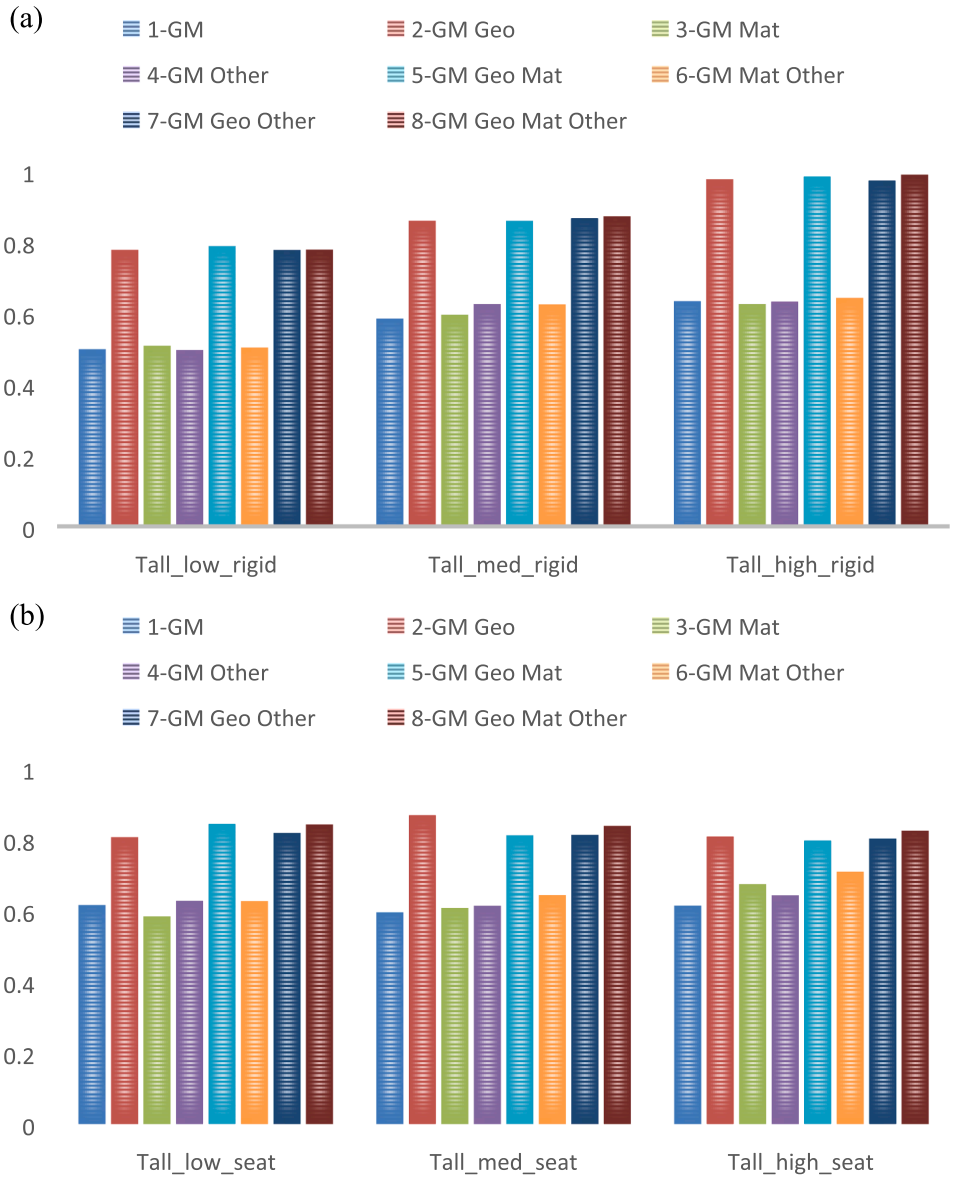

Fig. 7. Comparison of the column response dispersions for tall bridges with various column height ratios; (a) rigid abutment bridges, (b) seat abutment bridges.

dispersion increases as the column height increases from normal to tall with the high column height ratio, in all eight scenarios of uncertainty sources. However, it is clear that in all bridge types, there is a gap between the results of models including uncertainty in the geometric parameters and those of excluding this type of uncertainty. Therefore, it is seen that the geometric factors produce an average of $\frac{100 * (0.75 - 0.45)}{0.45} = 67\%$ higher variation in the responses.

In the case of seat abutment bridges (Fig. 8b), there is still an average of 27% gap between the results of models with and without the uncertainty in the geometric parameters but in this case, increasing the column height does not significantly alter the responses.

Fig. 9 elaborates the variations of bridge column responses for all considered bridge types. This Fig. evaluates the results when each source of uncertainty is added to the randomness associated with the ground motions. As shown, the values increases between 0.15 (for the normal bridge with seat abutment) to 0.35 (for the tall bridge with rigid abutment and high column ratio) when the uncertainties of geometric characteristics are added to the ground motion uncertainty. Although adding GEO variables changes dispersion values noticeably, combining additional variables (i.e. scenarios 5, 7, and 8) such as MAT and OTHERS factors changes the responses slightly. Hence, among the studied sources, GEO plays a major role in defining the bridge responses and ignoring the impact of geometric parameters in the seismic analysis of bridges can alter the conclusions significantly.

4. Comparative analysis of bridge fragility parameters

The seismic vulnerability evaluation of bridges facilitates post-earthquake emergency responses and determines suitable retrofit strategies. This assessment can be performed by implementing a

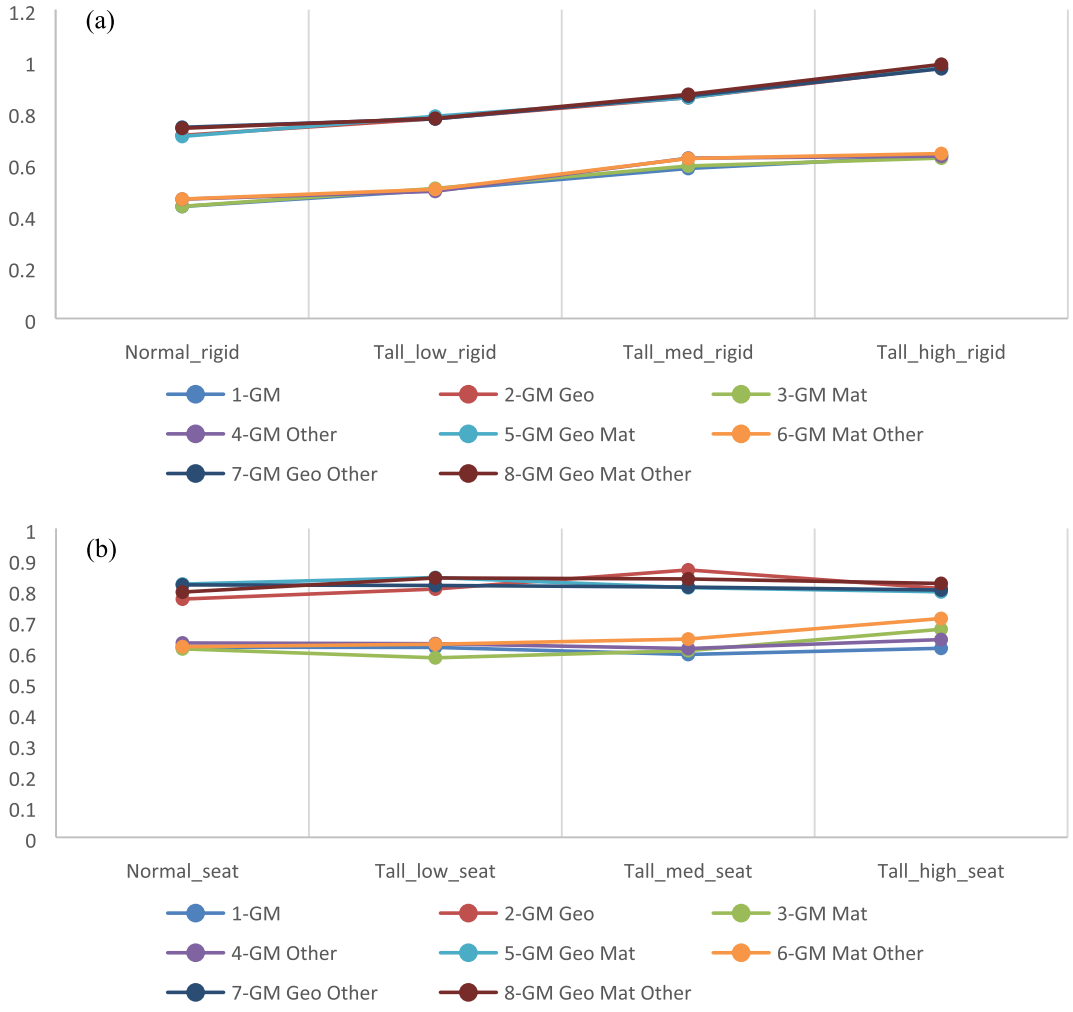

Fig. 8. Comparison between the dispersion values of the bridge column responses of normal and tall bridges.

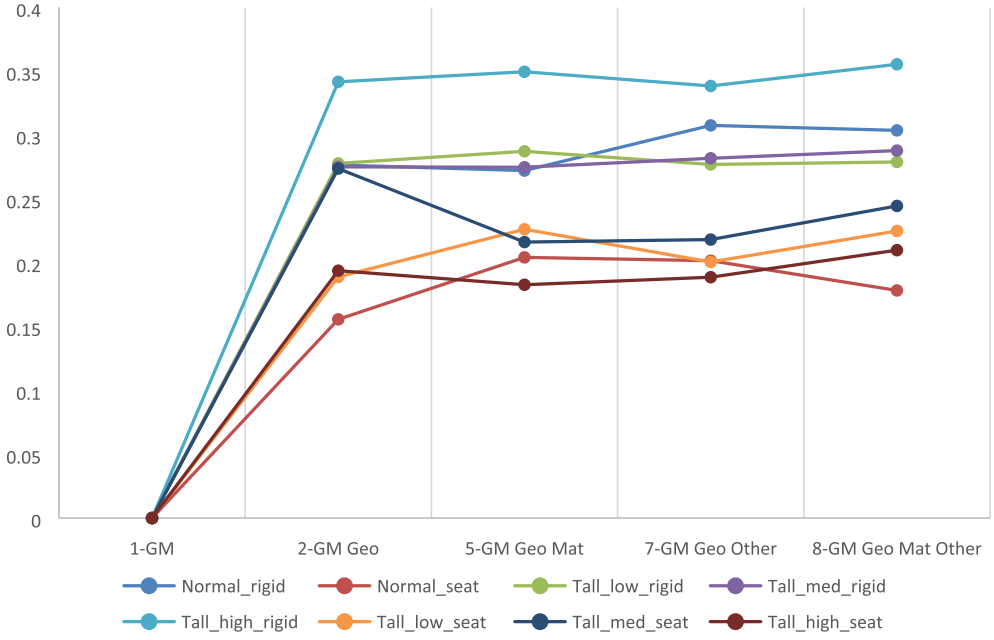

Fig. 9. Variation of the column response dispersion when GEO, MAT, and OTHERS randomness is added to the model including GM uncertainty.

Table 8
Qualitative damage levels for the bridge components (also found in Soleimani [28]).

Damage Levels	CDT-0	CDT-1	CDT-2	CDT-3
Description of damage	Aesthetic damage	Repairable minor functional damage	Repairable major functional damage	Component replacement

Table 9
Description of different damage states for the bridge system (also found in Soleimani [28]).

	Bridge system damage levels			
	BSST-0 Slight	BSST-1 Moderate	BSST-2 Extensive	BSST-3 Complete
Shake Cast Inspection Priority levels	Low	Medium	Medium-High	High
Likely Immediate Post-Event Traffic State	Open to normal public traffic – No Restrictions	Open to Limited public traffic – speed/weight/lane restrictions	Emergency vehicles only – speed/ weight/lane restrictions	Closed (until shored/braced) – potential for collapse
Traffic Operation				
Closure/detour needed	Very unlikely	Unlikely	Likely	Very Likely
Traffic restrictions needed	Unlikely	Likely	Very Likely	Very Likely
Emergency Repair				
Shoring/bracing needed	Very Unlikely	Unlikely	Likely	Very Likely
Roadway levelling needed	Unlikely	Likely	Very Likely	Very Likely
Primary Components	CDT-0 to 1	CDT-1 to 2	CDT-2 to 3	Above CDT-3
Secondary Components	CDT-0	CDT-1	NA	NA

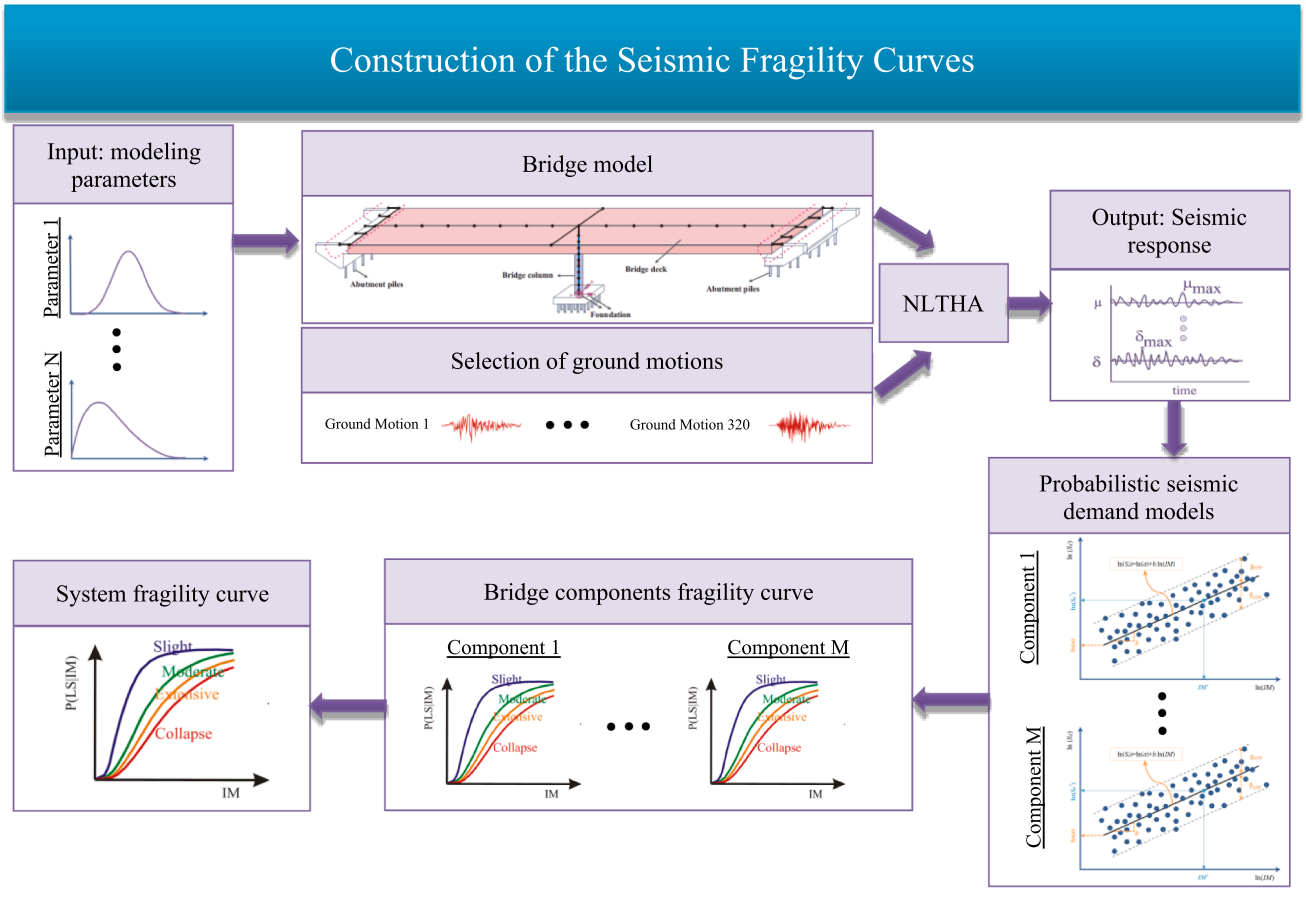

Fig. 10. Illustration of the steps for generating fragility curves.

Table 10
The assigned nomenclature for bridges with various configurations.

Bridge design era	No. of columns per bent	Abutment type	Nomenclature
Pre-1970	Single column	Rigid	SC-Rg-E1
	Single column	Seat	SC-St-E1
	Two columns	Rigid	TC-Rg-E1
	Two columns	Seat	TC-St-E1
	Multiple columns	Rigid	MC-Rg-E1
	Multiple columns	Seat	MC-St-E1
1970–1990	Single column	Rigid	SC-Rg-E2
	Single column	Seat	SC-St-E2
	Two columns	Rigid	TC-Rg-E2
	Two columns	Seat	TC-St-E2
	Multiple columns	Rigid	MC-Rg-E2
	Multiple columns	Seat	MC-St-E2
Post-1990	Single column	Rigid	SC-Rg-E3
	Single column	Seat	SC-St-E3
	Two columns	Rigid	TC-Rg-E3
	Two columns	Seat	TC-St-E3
	Multiple columns	Rigid	MC-Rg-E3
	Multiple columns	Seat	MC-St-E3

probabilistic approach in the form of fragility curves for the bridge components and the bridge system. This section evaluates the bridge fragility at four different damage states: slight, moderate, extensive, and complete. General descriptions of various levels of damage for the bridge components (i.e., Component Damage Threshold (CDT)) and the bridge system (i.e., Bridge System State Threshold (BSST)) are given in Table 8 and Table 9, using an approach from Soleimani [28] where the details of limit states can be found.

At a chosen intensity measure, the probability that the seismic demand (D) of a component exceeds its capacity (C) can be assessed through fragility curves. Assuming a lognormal distribution of demand and capacity [40,41] in conjunction with the first order reliability theory, the probability of reaching or exceeding a specific damage state for a particular component is estimated as

$$P[D > C|IM] = \Phi\left[\frac{\ln(S_D/S_c)}{\sqrt{\beta_{D|IM}^2 + \beta_C^2}}\right] \quad (4)$$

where S_D represents the median estimate of the demand, S_C is the median estimate of the capacity, $\beta_{D/IM}$ represents the dispersion of the demand, β_C is the dispersion of the capacity, and $\Phi(\bullet)$ corresponds to the standard normal cumulative distribution function.

Fig. 10 illustrates the process for generating fragility curves. The required demand parameters S_D and $\beta_{D/IM}$ for each bridge component are estimated from the PSDMs, and the corresponding capacity parameters are obtained from the limit states.

The results of the fragility analysis for the bridge models selected for the scope of this study are presented in the following section. For simplicity, the nomenclature is assigned to the tall bridges as given in Table 1 in Section 2, according to the irregularity ranges. Also, in the discussion of the results, BM stands for the base models, which are regular bridge models with normal column height. In addition to the irregularity parameters, the selected box-girder bridges for the fragility analysis are different in several configurations. Therefore, an additional nomenclature list based on various design eras, abutment types, and the number of columns per bent is provided in Table 10.

The components and system fragility curves for each specific bridge are generated using the explained methodology and including all the four sources of uncertainty mentioned in the previous section. The median (λ) and dispersion (ζ) of the generated fragility curves are given in Table 11. Then, the fragility values of tall bridges are compared to the fragility values of the base models as presented in Fig. 11.

The results shown in Table 11 and Fig. 11 illustrate that, for the three design eras, as the column height increases, the median fragility values decrease, which leads to higher seismic vulnerability. In the pre-1970 era, the variability between the medians of regular bridges and the tall class of bridges is higher at the higher levels of damage. However, this variation is constant for the 1970–1990 era. The difference between the medians is negligible at the slight damage state for the 1970–1990 and post-1990 eras. For bridges designed after 1990, the medians show higher variation at the complete damage level than at the other levels. On the other hand, the dispersion increases across the levels of irregularity. Compared to the dispersion of the regular bridges, all tall classes have higher dispersions for the pre-1970 era, while there is a slight decrease in the MTL and VTL dispersion values. In general, for each design era, the dispersion values of different bridge classes are in a similar range.

It is seen from the results that, for all bridge configurations, bridges designed post-1990 and pre-1970 demonstrate the least and the most vulnerability, respectively. Also, bridges designed between 1970 and 1990 are less vulnerable than bridges designed before 1970. The observed enhanced seismic performance of bridges designed more recently is attributable to considerable improvements in the seismic bridge design codes following the 1971 San Fernando and the 1989 Loma Prieta earthquakes. The difference between the vulnerability of recently-designed bridges and older bridges is more noticeable at higher degrees of irregularity (e.g., extremely tall bridges). However, the difference between the median fragilities of bridges designed during 1970–1990 and after 1990 is small, even for extremely tall and very tall bridges.

The fragility parameters for very tall bridges with various configurations are presented in Table 12. A comparison of the results for the

Table 11
Fragility parameters for the tall bridge types (specifications: multi-span continuous concrete box-girder bridges with seat abutments, single column per bent, and circular column cross-sections).

Bridge design era	Bridge type	BSST-0		BSST-1		BSST-2		BSST-3	
		λ	ζ	λ	ζ	λ	ζ	λ	ζ
Pre-1970	BM	0.102	0.499	0.200	0.488	0.382	0.489	0.540	0.485
	MTL	0.078	0.509	0.140	0.525	0.247	0.531	0.342	0.519
	VTL	0.059	0.528	0.103	0.540	0.174	0.530	0.235	0.535
	ExTL	0.049	0.561	0.087	0.566	0.148	0.566	0.206	0.568
1970–1990	BM	0.100	0.660	0.515	0.651	0.957	0.802	1.343	0.809
	MTL	0.071	0.610	0.374	0.549	0.832	0.736	1.236	0.746
	VTL	0.046	0.658	0.256	0.627	0.637	0.789	0.965	0.858
	ExTL	0.037	0.686	0.207	0.673	0.580	0.824	0.870	0.882
Post-1990	BM	0.095	0.651	0.515	0.653	1.296	0.772	2.052	0.770
	MTL	0.069	0.605	0.373	0.562	0.990	0.675	1.543	0.651
	VTL	0.045	0.658	0.256	0.626	0.707	0.735	1.068	0.693
	ExTL	0.037	0.682	0.206	0.672	0.602	0.784	0.925	0.809

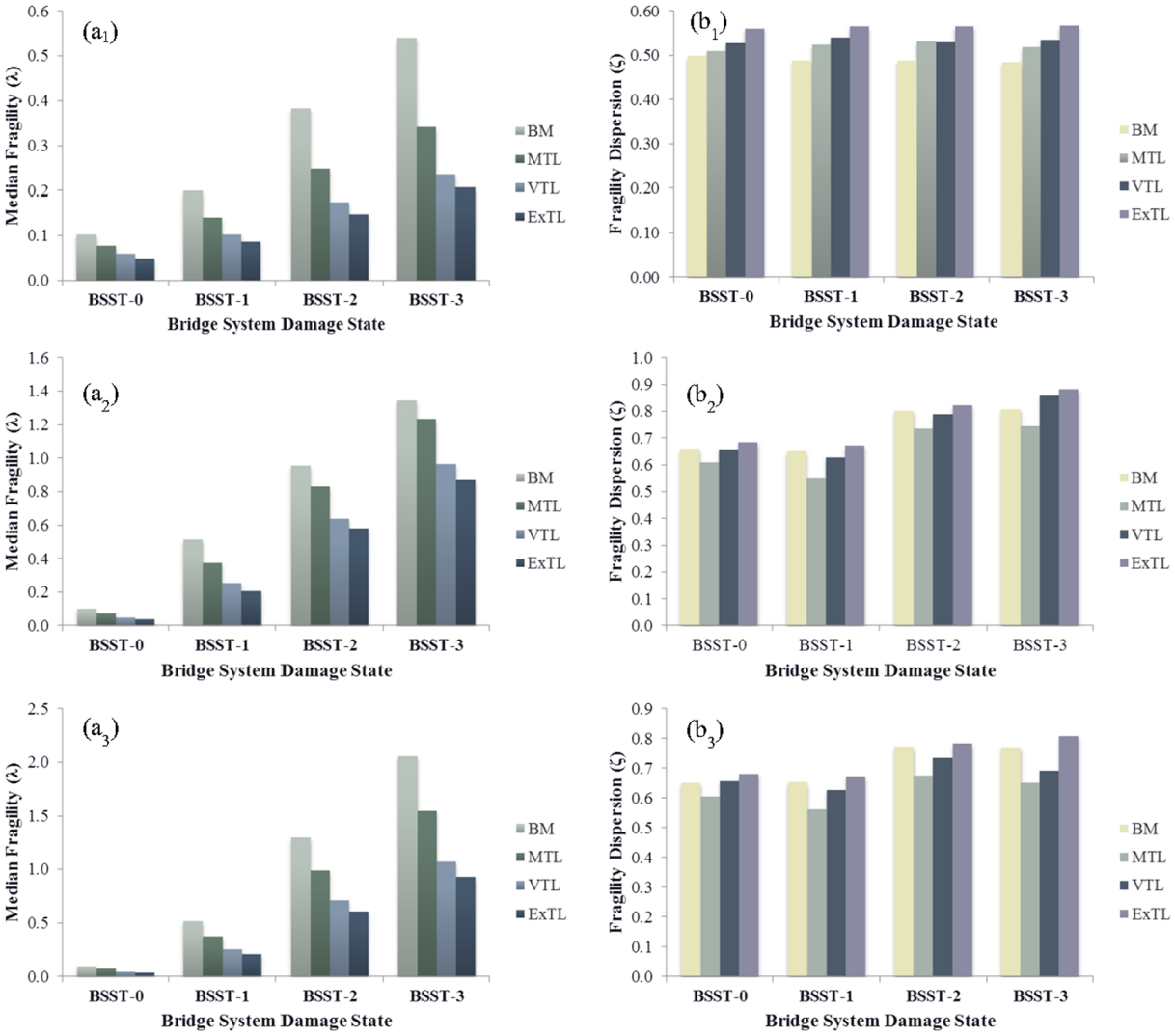

Fig. 11. Comparison of the median and dispersion of the bridge system fragility curves for the tall bridge types: (1) pre-1970 design era; (2) 1970–1990 design era; (3) post-1990 design era.

Table 12
Fragility parameters for the tall bridge types (specifications: multi-span continuous concrete box-girder bridges with circular column cross-sections and various abutment types and number of columns per bent).

Bridge type*	BSST-0		BSST-1		BSST-2		BSST-3	
	λ	ζ	λ	ζ	λ	ζ	λ	ζ
SC-Rg-E2	0.076	0.597	0.323	0.557	1.328	1.107	1.975	1.106
SC-St-E2	0.046	0.658	0.256	0.627	0.637	0.789	0.965	0.858
TC-Rg-E2	0.025	0.93	0.225	1.134	1.703	0.623	2.479	0.649
TC-St-E2	0.038	0.582	0.199	0.581	0.502	0.68	0.744	0.679
MC-Rg-E2	0.042	0.598	0.227	0.668	1.167	1.069	1.595	1.073
MC-St-E2	0.02	0.744	0.177	0.67	0.481	0.838	0.747	0.889
SC-Rg-E3	0.077	0.611	0.326	0.554	1.967	1.12	3.374	1.099
SC-St-E3	0.045	0.658	0.256	0.626	0.707	0.735	1.068	0.693
TC-Rg-E3	0.025	0.917	0.227	1.126	2.509	0.751	4.687	0.854
TC-St-E3	0.038	0.584	0.194	0.571	0.529	0.639	0.788	0.635
MC-Rg-E3	0.042	0.597	0.227	0.67	1.585	1.073	2.387	1.043
MC-St-E3	0.019	0.753	0.178	0.674	0.538	0.782	0.831	0.797

* Refer to Table 10 for the nomenclature.

seat and rigid abutment types shows that, for bridges with single, two, and multiple columns per bent, the fragility median difference is minor at the slight and moderate damage states, while major differences are observed at the extensive and complete damage states. This is more noticeable for bridges with two columns per bent. As an example, at BSST-3, the medians for TC-Rg-E3 and TC-St-E3 are 4.687 and 0.788 (i.e., 83.2% reduction), respectively while the medians for MC-Rg-E3 and MC-St-E3 are 2.387 and 0.831 (i.e., 65.2% reduction), respectively (Fig. 12). It is seen from Fig. 13 that the median changes among various numbers of columns per bent are negligible at BSST-0. It is also seen that at BSST-1, tall bridges with multi-column bents are more vulnerable than those with single column bents.

To assess the impact of the column height ratio on the resulting fragility curves, Fig. 14 shows a sample of the fragility curves constructed for the four levels of damage corresponding to slight, moderate, extensive, and complete. It is apparent that the column height has a significant impact on the fragilities at the moderate, extensive, and complete damage states (i.e., BSST-1, BSST-2, and BSST-3). More variations are observed for the extensive and complete damage states, at which the increase in the vulnerability is more noticeable between the

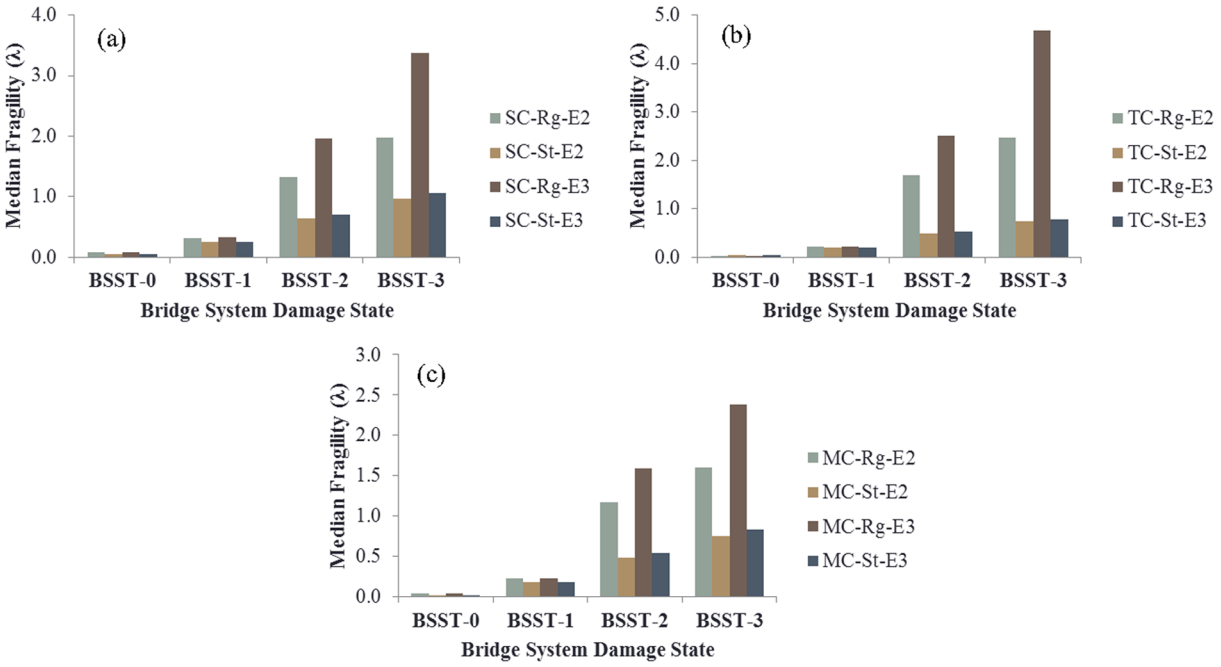

Fig. 12. Comparison of the median system fragilities of tall bridges based on various abutment types; (a) single column per bent; (b) two columns per bent; (c) three columns per bent.

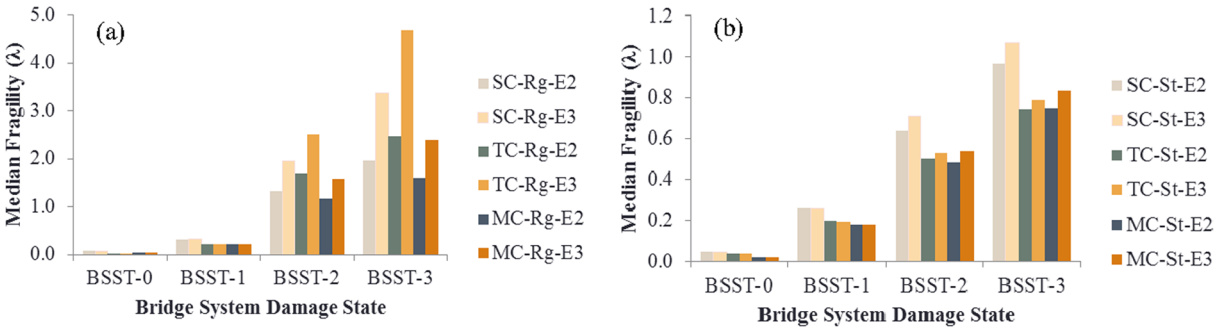

Fig. 13. Comparison of the median system fragilities of tall bridges based on the different number of columns per bent: (a) rigid diaphragm abutment; (b) seat type abutment.

regular bridge model (BM) and the MTL, and also between the MTL and the VTL. However, the increase rate is lower between the VTL and the ExTL. Similarly, at BSST-0, the fragility curve of the ExTL is very close to that of the VTL.

5. Conclusions

Fragility analysis is a powerful tool for the reliability and risk assessment of structures and is extensively applied to predict the extent of probable seismic damage to bridges with standard configurations. Identifying the most influential types of uncertainties among the entire random input variables is crucial in the process of demand analysis. Furthermore, a quantitative measure of the uncertainty that is involved in the process of developing probabilistic seismic demand models and the fragility curves was missing in the previous works. Therefore, a separate study was needed to solely focus on this issue and address this deficiency. Also, the seismic response and performance of tall bridges have not been deeply studied, and hence there was a need to further assess the seismic performance of this bridge configuration. This paper assessed the influence of major sources of uncertainties and quantified their impacts on bridge vulnerability. The sensitivity of the uncertainty in bridge responses was investigated with respect to the uncertainty in different types of parameters that are involved in the modeling and analysis of bridges.

This study considered the material uncertainty along with the uncertainties associated with the ground motions and geometric attributes pertinent to concrete box-girder bridges. In each step, the uncertainty of only one type of parameters has been included in the model and the other remaining parameters have been considered as deterministic. Adding each source of uncertainty increased the variation in the values of engineering demand parameters of bridges. However, the uncertainties associated with the geometric attributes showed the highest influence on the seismic demands of considered bridges. On the other hand, the material and other sources of uncertainties changed the

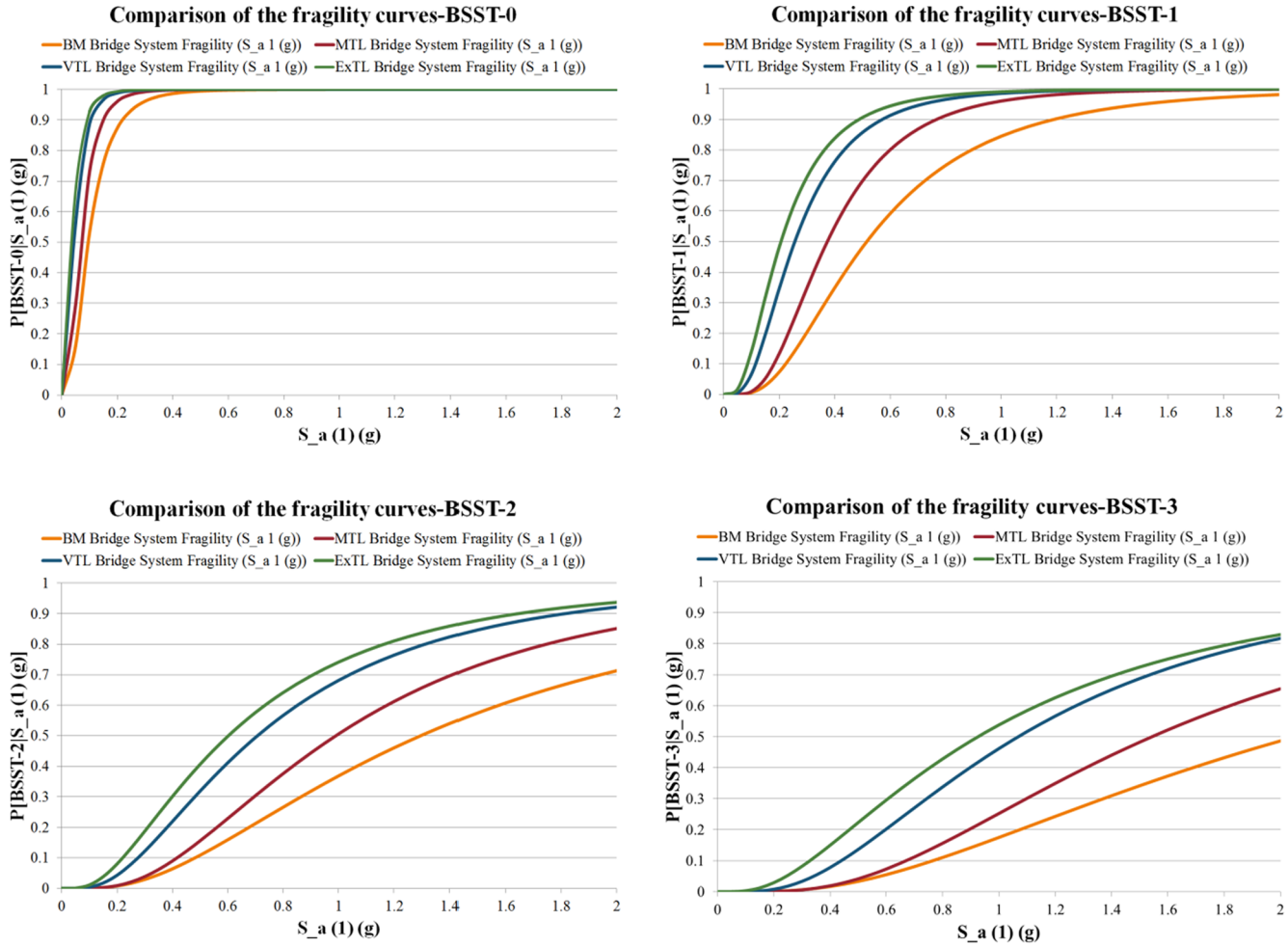

Fig. 14. Comparison of the system fragility curves for the class of tall bridges (specifications: SC-St-E3 and circular column cross-sections).

response variations slightly. The findings showed that the geometric attributes added more variation to the responses of bridges with tall column heights than those of bridges with typical column heights.

Various combinations of the mentioned sources of uncertainties have been added to the bridge models and the contribution of each combination on the dispersion of the bridge response was assessed for normal and tall bridges with rigid and seat abutments. Although comparing the results for bridges with rigid and seat abutments using the Pareto plots revealed that the dispersion of bridge responses are pretty similar, the response dispersion of rigid type bridges was higher than those of the seat type bridges for the combinations including geometric random features. Normal and tall bridges with rigid and seat abutments are assessed in this paper and reveal that, in most cases, higher uncertainty was involved in the vulnerability analysis of seat bridge types. As the column height ratio increased from low to high, the dispersion of the bridge seismic response also increased. The patterns of the bridge responses and the influence of the different kinds of uncertainties were similar for the various ground motion scales including PGA, Sa(0.3 s), Sa(0.2 s), and Sa(1.0 s).

Additionally, while many researchers have focused on the fragility analysis of bridges with normal column heights, only a few have analyzed seismic damage of tall bridges. Therefore, this paper attempted to provide insight regarding the demand and fragility analysis of the class of tall concrete box-girder bridges to better understand the performance of the class of tall bridges. Overall, the produced fragility analysis results indicated the higher vulnerability of the class of tall bridges compared to the normal bridges. Based on the results, the column height had a significant impact on the fragilities at the moderate, extensive, and complete damage states. The increase in the vulnerability was more noticeable between the normal bridges and the moderately tall bridges, and also between the moderately tall bridges and the very tall bridges.

This study assessed the vulnerability of bridges with various types of attributes including two abutment types, three design eras, and three categories for the number of columns per bent. Comparison of the responses of bridges with single, two, multiple column heights indicated that the differences between the median fragilities were minor at slight and moderate damage states. In all design eras, as the column height increased from normal to extremely tall, the median fragility value decreased which is indicative of the higher seismic vulnerability of the bridge. For bridges designed before 1970, the variability in the median fragility was higher in higher degrees of damage. The impact of the improvements in the bridge design codes was clear in the results particularly in the higher levels of column heights. The bridges designed before 1970 and those designed after 1990 showed the most and the least vulnerability, respectively.

Declaration of Competing Interest

The authors declare that there is no conflict of interest.

References

[1] Shinozuka M, Feng MQ, Lee J, Naganuma T. Statistical analysis of fragility curves. J. Eng. Mech.-ASCE 2000;126:1224–31.
[2] Nielson BG. Analytical fragility curves for highway bridges in moderate seismic zones. Atlanta: School of Civil and Environmental Engineering, Georgia Institute of

Technology; 2005.
[3] Yu O, Allen DL, Drenvich VP. Seismic vulnerability assessment of bridges on earthquake priority routes in Western Kentucky. Lifeline Earthquake Eng. 1991:817–26.
[4] Hwang H, Jernigan JB, Lin YW. Evaluation of seismic damage to Memphis bridges and highway systems. J. Bridge Eng. 2000;5:322–30.
[5] Gardoni P, Mosalam KM, der Kiureghian A. Probabilistic seismic demand models and fragility estimates for RC bridges. J. Earthquake Eng. 2003;7:79–106.
[6] Zhong J, Gardoni P, Rosowky D, Haukaas T. Probabilistic seismic demand models and fragility estimates for reinforced concrete bridges with two-column bents. J. Eng. Mech. 2008;134:495–504.
[7] Choi E, DesRoches R, Nielson B. Seismic fragility of typical bridges in moderate seismic zones. Eng. Struct. 2004;26(2):187–99.
[8] Mackie KR, Stojadinovic B. Fragility basis for California highway overpass bridge seismic decision making. Pacific Earthquake Eng. Res. Center 2005.
[9] Jeong S, Elnashai A. Probabilistic fragility analysis parameterized by fundamental response quantities. Eng. Struct. 2007;29:1238–51.
[10] Padgett JE, DesRoches R. Methodology for the development of analytical fragility curves for retrofitted bridges. Earthquake Eng. Struct. Dyn. 2008;37(8):1157–74.
[11] Zhang J, Huo YL. Evaluating effectiveness and optimum design of isolation devices for highway bridges using the fragility function method. Eng. Struct. 2009;31:1648–60.
[12] Ramanathan KN. “Next generation seismic fragility curves for California bridges incorporating the evolution in seismic design. Philosophy 2012.
[13] Buckle IG. The Northridge, California earthquake of January 17 1994. Performance of highway bridges, NCEER-94-0008. 1994.
[14] Yashinsky M, Oviedo R, Ashford SA, Fargie-Gabaldon L, Hube M. Performance of highway and railway structures during the February 27, 2010. Maule Chile earthquake EERI/PEER/FEMA bridge team report. 2010.
[15] Kawashima K, Unjoh S, Hoshikuma J, Josa K. Damage of transportation facility due to 2010 Chile earthquake. Bridge Team Dispatched by Japan Society of Civil Engineers. 2010.
[16] Soleimani F, Yang C, DesRoches R. The effect of superstructure curvature on the seismic performance of box-girder bridges with in-span hinges. Struct. Congress 2017:469–80.
[17] Q. Zheng and L. Wenhua, “Seismic design of high piers for mountain bridges,” 2006.
[18] Ang AS, De Leon D. Modeling and analysis of uncertainties for risk-informed decisions in infrastructures engineering. Struct. Infrastruct. Eng. 2005;1(1):19–31.
[19] Ang AH-S, Tang WH. Probability concepts in engineering: emphasis on applications in civil & environmental engineering. 2nd ed. New York: Wiley; 2007.
[20] Der Kiureghian A, Ditlevsen O. Aleatory or epistemic? Does it matter? Struct. Saf. 2009;31(2):105–12.
[21] Zhang R, Mahadevan S. Model uncertainty and Bayesian updating in reliability-based inspection. Struct. Saf. 2000;22(2):145–60.
[22] Biondini F, Frangopol D. Probabilistic limit analysis and lifetime prediction of concrete structures. Struct. Infrastruct. Eng. 2008;4(5):399–412.
[23] Goulet J-A, Der Kiureghian A, Li B. Pre-posterior optimization of sequence of measurement and intervention actions under structural reliability constraint. Struct. Saf. 2015;52:1–9.
[24] Biondini F, Frangopol DM. Life-cycle performance of deteriorating structural systems under uncertainty. J. Struct. Eng. 2016;142(9).
[25] Mackie KR, Nielson BG. Uncertainty quantification in analytical bridge fragility curves. In TCLEE 2009: Lifeline Earthquake Engineering in a Multihazard Environment. 2009. p. 1–12.
[26] Wang L, Ma Y, Zhang J, Zhang X, Liu Y. Uncertainty quantification and structural reliability estimation considering inspection data scarcity. ASCE-ASME J. Risk Uncertainty Eng. Syst. Part A: Civil Eng. 2015;1(2):04015004.
[27] Soleimani F, Vidakovic B, DesRoches R, Padgett J. Identification of the significant uncertain parameters in the seismic response of irregular bridges. Eng. Struct. 2017;141:356–72.
[28] Soleimani F. Fragility of California bridges-development of modification factors. Doctoral dissertation, Georgia Institute of Technology; 2017.
[29] Mazzoni S, McKenna F, Scott MH, Fenves GL. OpenSees command language manual. Pacific Earthquake Eng. Res. (PEER) Center 2006.
[30] Soleimani F, Mangalathu S, DesRoches R. A comparative analytical study on the fragility assessment of box-girder bridges with various column shapes. Eng. Struct. 2017;153:460–78.
[31] Soleimani F, Mangalathu S, DesRoches R. Seismic resilience of concrete bridges with flared columns. Procedia Eng. 2017;199:3065–70.
[32] Soleimani F, McKay M, Yang CW, Kurtis KE, DesRoches R, Kahn L. Cyclic testing and assessment of columns containing recycled concrete debris. ACI Struct. J. 2016;113(5):1009.
[33] Mander JB, Priestley MJN, Park R. Theoretical Stress-Strain Model for Confined Concrete. J. Struct. Eng. 1988;ASCE:1804–25.
[34] M. Menegotto and P. E. Pinto, “Method of Analysis for Cyclically Loaded RC Frames Including Changes in Geometry and Non-elastic Behaviour of Elements Under Combined Normal Force and Bending,” 1973.
[35] Filippou FC, Popov EP, Bertero VV. Effects of bond deterioration on hysteretic behavior of reinforced concrete joints. Washington DC: SAC Joint Venture; 1983.
[36] Shamsabadi A, Yan L. Closed-form force-displacement backbone curves for bridge abutment-backfill systems. Proceedings of the Geotechnical Earthquake Engineering and Soil Dynamics IV Congress. 2008.
[37] Muthukumar S, DesRoches R. A Hertz contact model with non-linear damping for pounding simulation. Earthquake Eng. Struct. Dyn. 2006;35(7):811–28.
[38] Baker JW, Lin T, Shahi SK, Jayaram N. New ground motion selection procedures and selected motions for the PEER transportation research program. Pacific Earthquake Engineering Research Center. 2011.
[39] Ayyub BM, Lai KL. Structural reliability assessment using latin hypercube sampling. Structural Safety and Reliability. 1989. p. 1177–84.
[40] Cornell C, Jalayer F, Hamburger R, Foutch D. Probabilistic basis for 2000 SAC federal emergency management agency steel moment frame guidelines. J. Struct. Eng. 2002;128(4):526–33.
[41] Song J, Ellingwood BR. Seismic reliability of special moment steel frames with welded connections: II. J. Struct. Eng. 1999;125(4):372–84.